Nonlinear Anisotropic Diffusion Filters for Wide Range Edge Sharpening

Steve Keeling and Rudolf Stollberger

- Motivation
- Perona-Malik Filters
- Proposed Widely Sharpening Filters
- Numerical Methods
- Computational Results

Basic Problem: Vascular segmentation/visualization.

First explain what you see here:

- Inject blood pooling contrast agent into patient.
  - Remains and distributes.
  - Unlike other more dissipative agents.
- Take 3D MR data set.
- How to visualize?
  - Serial viewing inconvenient.
  - Threshold rendering inadequate.
- Here is maximum intensity projection.
  - Each point is maximum intensity along line.
  - Separate images are different projections.
- MIP is stunning but complicated.
- Arteries or veins?
- Need tool for virtual investigations.
- Virtual angiography.

Motivation

- New blood pooling contrast agents.
- Serial viewing inconvenient.
- Maximum intensity projections.
- Distinguish arteries and veins.
- Ultimate Goal: Virtual Angiography.
- Problems necessitating preprocessing:
  - Rapid access, low signal/noise: noise filtering.
  - High RF inhomogeneity: trend filtering.
- Denoising, deblurring, segmentation:

  edge sharpening.

What is an edge?

- In 1D: u_{xx} changes sign.

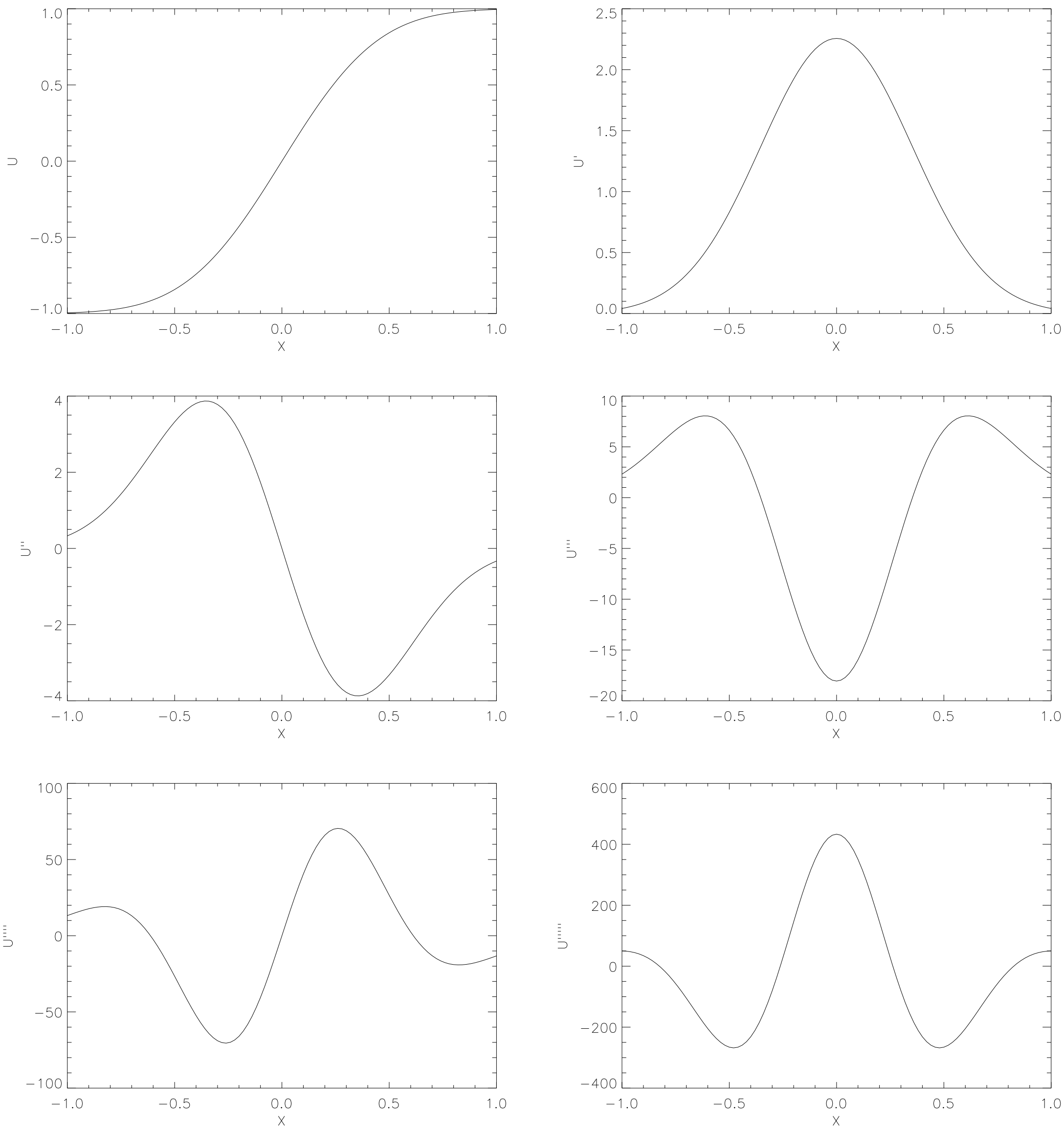

- In 2D: u_{nn} (or $\nabla u \cdot H_u \cdot \nabla u$) changes sign.

- In 2D:
  - u_{nn} (or $\nabla u \cdot H_u \cdot \nabla u$) changes sign.
  - Consider: $u(x, y) = -x^2(1-x)^2(1-y)^2$

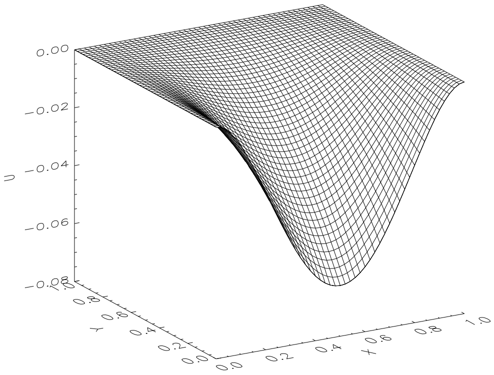

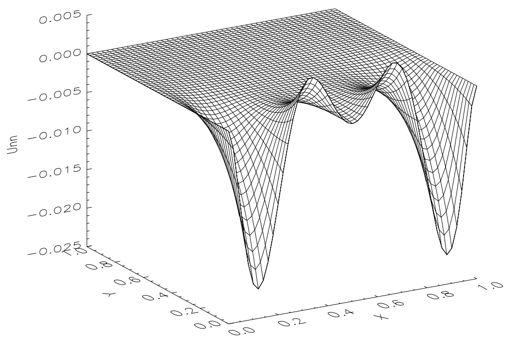

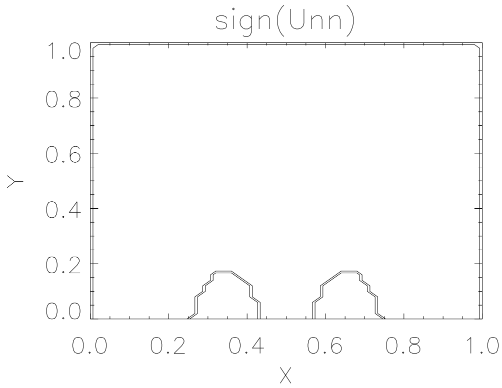

  - Best: eigenvalues of H_u change sign.
  - Edge detector study [Rudin, 1987].
  - u_{nn} used [Osher & Rudin, 1990].
  - Steeper slopes bring u_{nn} edges closer to level sets.

Models for Blurring and Sharpening

- Blurring: forward diffusion

$$\begin{cases} \partial_t u = +\nabla^2 u \\ u(0) = u_0 \end{cases}$$

Consider: $u(x,t) = \mathrm{Erf}\left(\dfrac{x}{2\sqrt{t}}\right)$

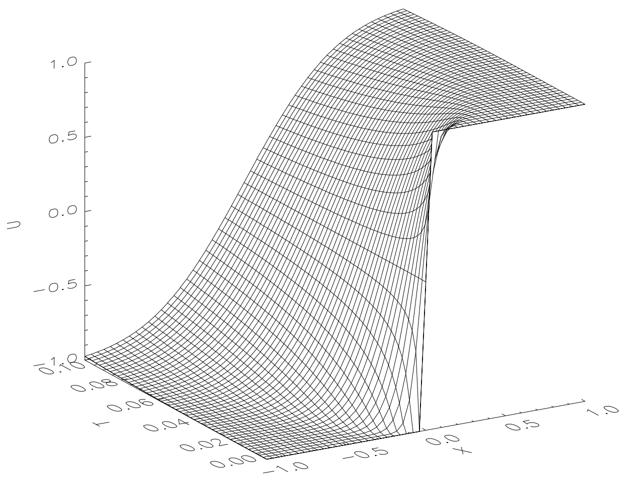

- Sharpening: backward diffusion

$$\begin{cases} \partial_t u = -\nabla^2 u \\ u(0) = u_0 \end{cases}$$

Backward diffusion unstable.

Approaches to Edge Enhancement

- Shock filtering [Osher & Rudin, 1990].

$$\begin{cases} \partial_t u = -|\nabla u| F(\mathcal{L}(u)) & F \to u_{nn} \\ u(0) = u_0 \end{cases}$$

  - Based on level set methods:

$$u(\boldsymbol{x}(t), t) = \text{constant}$$

$$\partial_t u + \nabla u \cdot \dot{\boldsymbol{x}} = 0$$

$$\frac{\nabla u \cdot \dot{\boldsymbol{x}}}{|\nabla u|} = F \quad \Rightarrow \quad \partial_t u = -|\nabla u| F$$

In 1D: $\partial_t u = -|u_x| u_{xx}$

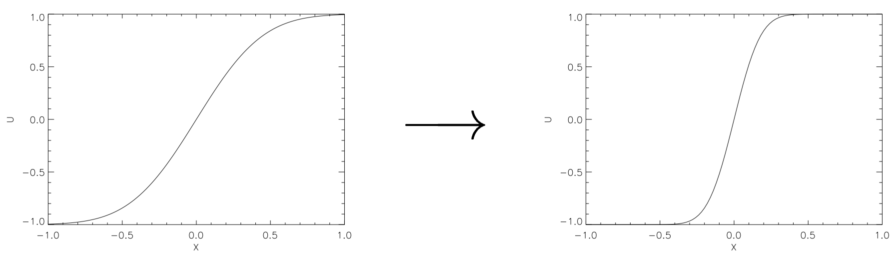

  - No tangential diffusion.
  - Only normal backward diffusion.
  - Consider radial function.
  - Shown to be well-posed! [Osher & Rudin, 1990]

Approaches to Edge Enhancement

- Shock filtering [Osher & Rudin, 1990].

$$\begin{cases} \partial_t u &= -|\nabla u| F(\mathcal{L}(u)) \qquad F \to u_{nn} \\ u(0) &= u_0 \end{cases}$$

  Based on level set methods. Well-posed!

- Variational Filtering.

$$\min_u J(u) = \int_P \phi(|\nabla u|)dx + \nu \int_P |u_0 - u|^2$$

  Optimality condition in steady state:

$$\begin{cases} \partial_t u &= \nabla \cdot \left(\phi'(|\nabla u|) \frac{\nabla u}{|\nabla u|} \right) + \nu(u_0 - u) \\ u(0) &= u_0 \end{cases}$$

  - Iterative methods approximate such evolution.
  - Shape of $\phi(s)$?
    - ▷ Gaussian [Tikhonov & Arsenin, 1977]

$$\phi(s) = \tfrac{1}{2}s^2$$

    - ▷ Total Variation (TV) [Rudin et al., 1992]

$$\phi(s) = s$$

    - ▷ Edge-Flat-Grey (EFG) [Ito & Kunisch, 1999]

$$\phi(s) = s^{p(s)} \qquad p(s) : 1 \to 2 \to 1$$

  - $\phi(s)$ convex for *image reconstruction.*

- ◦ $\phi(s)$ concave for *edge sharpening* [Nördstrom, 1990]
  - ▷ Normal and tangential diffusion decomposition:

$$\begin{aligned} \partial_t u &= \nabla \cdot \left(\phi'(|\nabla u|) \frac{\nabla u}{|\nabla u|} \right) + \nu(u_0 - u) \\ &= \phi'' u_{nn} + \frac{\phi'}{|\nabla u|}(\nabla^2 u - u_{nn}) + \nu(u_0 - u) \end{aligned}$$

  - ▷ Need $\phi''(s) < 0$ for backward diffusion.
- ◦ Reaction term:
  - ▷ Holds u near u_0.
  - ▷ Contributes to staircasing [Benhamouda, 1994].
  - ▷ Choose ν or $t_{\max}$.

Perona-Malik Filters

- Nonlinear diffusion:

$$\begin{cases} \partial_t u = \nabla \cdot (g(|\nabla u|)\nabla u) & g(s) = \phi'(s)/s \\ u(0) = u_0 \end{cases}$$

  Flux: $\Phi = |g(|\nabla u|)\nabla u|$, i.e., $\Phi(s) = sg(s)$.

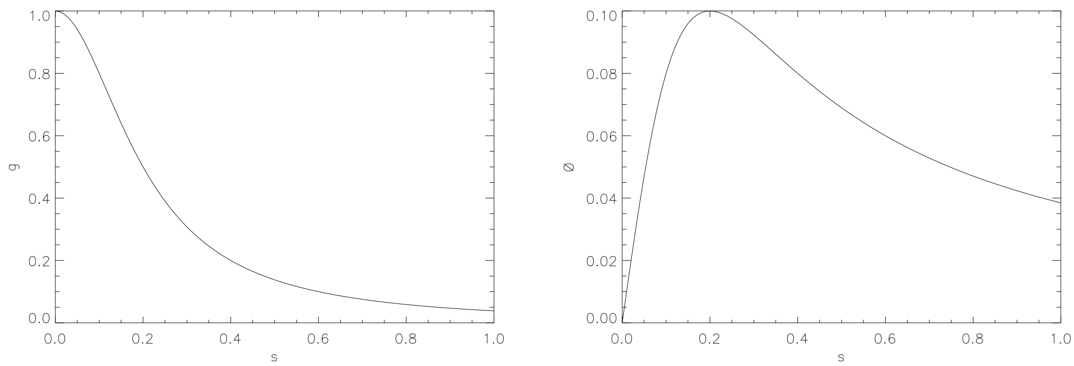

- g decreasing:
  - ▷ More diffusion for smaller $|\nabla u|$.
  - ▷ Less diffusion for larger $|\nabla u|$.
- g bell-shaped, Φ increasing then decreasing:

$$\partial_t u = \Phi' u_{nn} + g(\nabla^2 u - u_{nn})$$

  - ▷ Tangential diffusion always forward.
  - ▷ Normal diffusion forward where Φ increasing.
  - ▷ Normal diffusion backward where Φ decreasing.
- Diffusion is anisotropic.

How Can This Work?

- Backward diffusion and well-posedness?
- Amplification of noise [Perona & Malik, 1987].
- Divergent solutions [You et al., 1996].
- Non-existence of weak solutions [Kichenassamy, 1997].
- Perona-Malik Paradox [Weickert, 1998]:
  - Poor continuum properties.
  - Numerical implementations appear stable!
- Perona-Malik Problems:
  - Only numerical instability: staircasing.
  - Sensitivity to parameters:
    - ▷ Narrow range of edge slopes sharpened.
    - ▷ Other edges staircased or smoothed.

Demonstration of Perona-Malik Edge Sharpening

- Weaker edge smoothed:

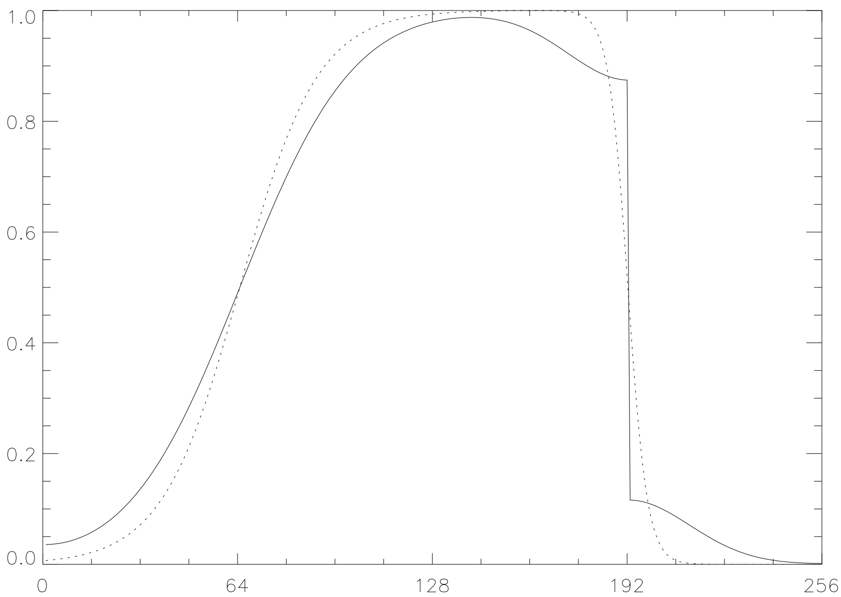

- Stronger edge staircased:

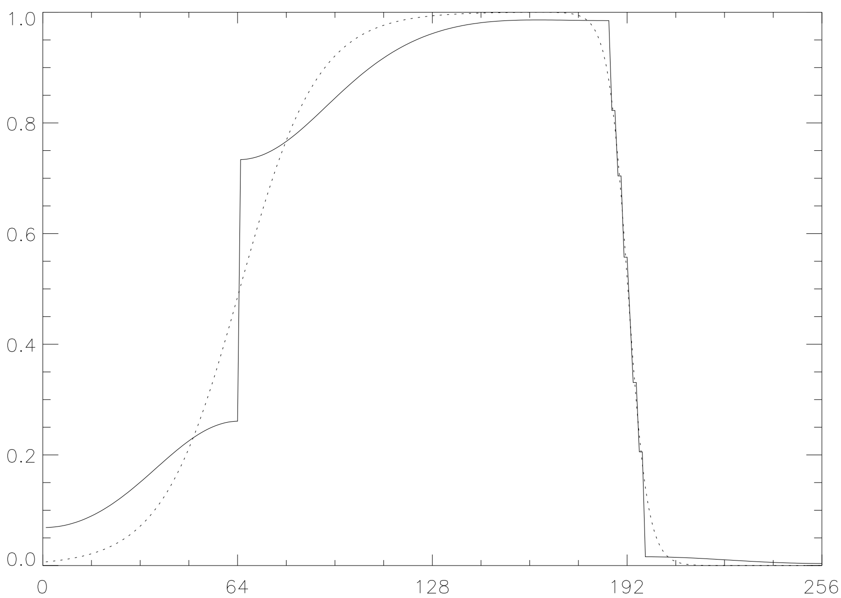

Perona-Malik Regularizations

- Discretization implicitly regularizes [Weickert, 1998].
- Spatial regularization [Catté et al., 1992]:

$$\partial_t u = \nabla \cdot (g(|\nabla u_\sigma|)\nabla u), \qquad u_\sigma = K_\sigma * u$$

  - Additional parameter: σ is noise scale.
  - Shown to be well-posed.
- Temporal regularization [Lions].
- Spatio-temporal regularization [Nitzberg & Shiota, 1992].
- Additional differential terms [Barenblatt et al., 1993].

Established Perona-Malik Diffusivities

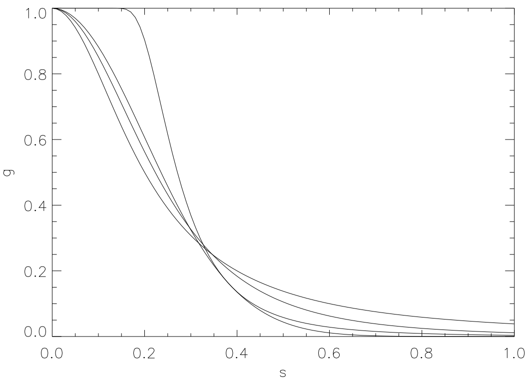

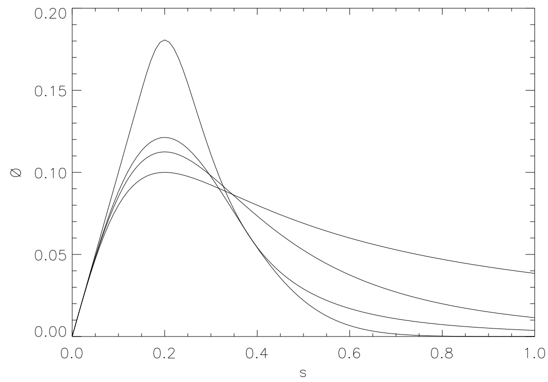

PM1: $\left[1+\left(\frac{s}{\lambda}\right)^2\right]^{-1}$ [Perona & Malik, 1987]

GR: $\left[1+\frac{1}{3}\left(\frac{s}{\lambda}\right)^2\right]^{-2}$ [Geman & Reynolds, 1992]

PM2: $\exp\left[-\frac{1}{2}\left(\frac{s}{\lambda}\right)^2\right]$ [Perona & Malik, 1987]

W: $1-\exp\left[-\gamma\left(\frac{s}{\lambda}\right)^{-4}\right]$ [Weickert, 1998]

- Φ increasing then decreasing: $\Phi'(\lambda)=0$.
- ϕ convex then concave: $\phi''(\lambda)=0$.
- Computational Preview:
  - ◦ More rapid decay:
    more durable sharpening over narrower range.
  - ◦ Less rapid decay:
    less durable sharpening over wider range.
- Analysis preview:
  sharpening for $\lambda \le |\nabla u| \le \chi$, where $\Phi''(\chi)=0$.

Proposed Widely Sharpening Filters

Test problem:

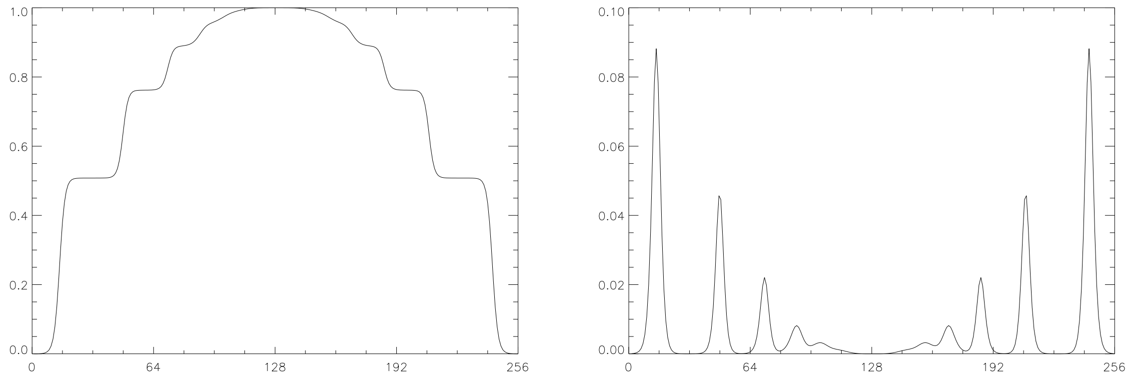

LEFT: u_0 with varying edge types, RIGHT: $|u_0'|$.

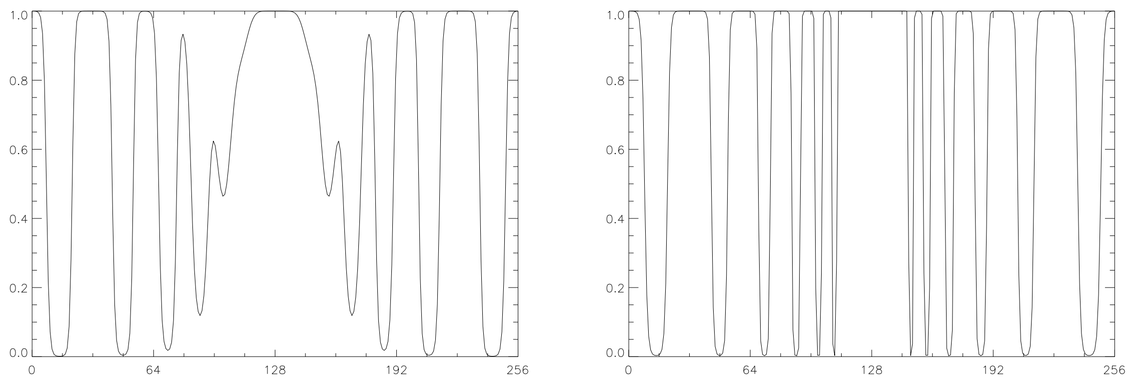

LEFT: PM1 $g(|u_0'|)$, RIGHT: idealized diffusivity.

- u_0 is sum of 6 functions: $a(1+bx^2)^{-c}$.
- Cannot use PM diffusivities to sharpen all edges.
- g reduces at edges but not uniformly.
- Two methods to fix:
  - Adjust λ locally,
  - Scale $|u_x|$ locally.
- Okay in 1D, but not robust in 2D.

Continuum Level Analysis

- 1D edge assumptions:
  - Even derivatives vanish: $u_{xx} = 0,\ u_{xxxx} = 0.$
  - Odd derivatives alternate in sign:

$$u_x > 0,\ u_{xxx} < 0,\ u_{xxxxx} > 0.$$

- Then for:

$$\begin{aligned} \partial_t u &= 0 && \\ \partial_t u_x &= \Phi' u_{xxx} > 0 && \text{need } \Phi' < 0 \\ \partial_t u_{xx} &= 0 && \\ \partial_t u_{xxx} &= 3\Phi'' u_{xxx}^2 + \Phi' u_{xxxxx} < 0 && \text{need } \Phi'' < 0. \end{aligned}$$

- Three edge classes:
  - Edges blurred: $|u_x| < \lambda \ \Rightarrow\ \Phi' > 0.$
  - Edges sharpened, turning rate locally max:

$$\lambda < |u_x| < \chi \ \Rightarrow\ \Phi' < 0, \Phi'' < 0.$$

  - Edges staircased, turning rate locally min:

$$|u_x| > \chi^+ \ \Rightarrow\ \Phi' < 0, \boxed{\Phi'' > 0}.$$

- In practice:
  - Different PM diffusivities can have same λ and χ but very different performance.
  - Best sharpening diffusivity depends on edge gradient profile.
  - Discretization alone gives edges of different slopes to edges with different heights.

Guided by Computational Experiments

- Need Φ' as uniformly negative as possible? Take:

$$\Phi'(s) = -1, \quad \Phi(s) = M - s, \quad g(s) = \frac{M - s}{s}.$$

- Okay in 1D, too much smoothing in 2D.
- Only dissipative mechanism is tangential:

$$\Phi'(s) = -1, \quad g(s) = \mathcal{O}\left(\frac{1}{s}\right).$$

- Tried $g(s) = \dfrac{1}{s^p}$:
  - $p > 2$ was unstable.
  - $p \approx 2$ looked good!
- Realized:

$$-1 = \frac{\Phi'(s)}{g(s)} = \frac{sg'(s) + g(s)}{g(s)} \quad \Rightarrow \quad g(s) = \frac{1}{s^2}.$$

Balanced Forward-Backward (BFB) diffusivity.

- *Balanced Forward-Backward* (BFB) diffusivity:

$$-1 = \frac{\Phi'(s)}{g(s)} = \frac{sg'(s) + g(s)}{g(s)} \quad \Rightarrow \quad g(s) = \frac{1}{s^2}.$$

- Simultaneous increase in both $|\Phi'|$ and g as $s \to 0$.
  - Possibly too much smoothing.
  - Possible enhancement of noise.
- Bring $|\Phi'|$ and g into balance gradually:

  $$-\frac{s}{\kappa + s} = \frac{\Phi'(s)}{g(s)} = \frac{sg'(s) + g(s)}{g(s)} \quad \Rightarrow \quad g(s) = \frac{1}{s(\kappa + s)}.$$

  Gradually Balanced Forward-Backward (GBFB) diffusivity.
- GBFB follows:
  - TV model for small s,
  - BFB model for large s.

Summary of Diffusivities

	$g(s)$	$\Phi'(s)$	$\Phi'(s)/g(s)$
G:	1	1	1
TV:	s^{-1}	0	0
BFB:	s^{-2}	$-s^{-2}$	-1
GBFB:	$[s(\kappa+s)]^{-1}$	$-(s+\kappa)^{-2}$	$-s/(\kappa+s)$
PM1:	$\left[1+\left(\frac{s}{\lambda}\right)^2\right]^{-1}$	$\dfrac{1-\left(\frac{s}{\lambda}\right)^2}{\left[1+\left(\frac{s}{\lambda}\right)^2\right]^2}$	$\dfrac{1-\left(\frac{s}{\lambda}\right)^2}{\left[1+\left(\frac{s}{\lambda}\right)^2\right]}$
PM2:	$\exp\left[-\frac{1}{2}\left(\frac{s}{\lambda}\right)^2\right]$	$\dfrac{1-\left(\frac{s}{\lambda}\right)^2}{\exp\left[\frac{1}{2}\left(\frac{s}{\lambda}\right)^2\right]}$	$1-\left(\dfrac{s}{\lambda}\right)^2$

- First three provide the basic models.
- PM's follow G for small s: $\Phi' > 0$, $\Phi''(0) = 0$.
- PM1 follows BFB for large s: $\Phi'/g \to -1$.
- PM's go convex to concave: $\phi'' = \Phi' > 0$ then < 0.
- BFB and GBFB globally concave: $\phi'' = \Phi' < 0$.
- Concave filters never follow G: no normal smoothing.

<u>Concave Filter Paradox</u>: remarkably stable and effective even with such limited dissipation.

Numerical Methods

First, spatial approximation for:

$$\partial_t u = \nabla \cdot (g(|\nabla u|)\nabla u)$$

Diagonal discretization:

$$2h^2[\nabla \cdot (g(|\nabla V|)\nabla U)]_{i,j} =$$

$$g_{i+\frac{1}{2},j+\frac{1}{2}}\left[U_{i+1,j+1} - U_{i,j}\right] - g_{i-\frac{1}{2},j-\frac{1}{2}}\left[U_{i,j} - U_{i-1,j-1}\right] +$$

$$g_{i-\frac{1}{2},j+\frac{1}{2}}\left[U_{i-1,j+1} - U_{i,j}\right] - g_{i+\frac{1}{2},j-\frac{1}{2}}\left[U_{i,j} - U_{i+1,j-1}\right]$$

where $g_{i+\frac{k}{2},j+\frac{l}{2}} = g(|\nabla V_{i+\frac{k}{2},j+\frac{l}{2}}|)$ and for $k, l = \pm 1$:

$$2[h|\nabla V|_{i+\frac{k}{2},j+\frac{l}{2}}]^2 = |V_{i+k,j+l} - V_{i,j}|^2 + |V_{i+k,j} - V_{i,j+l}|^2.$$

Graphically:

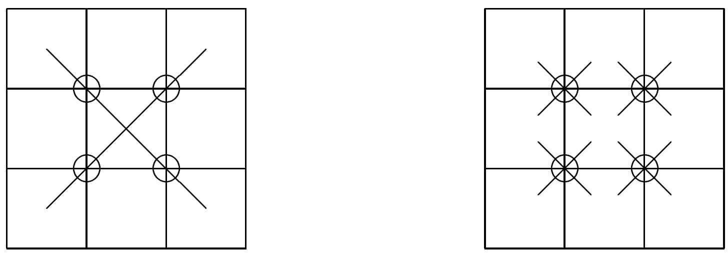

Horizontal-vertical too dissipative:

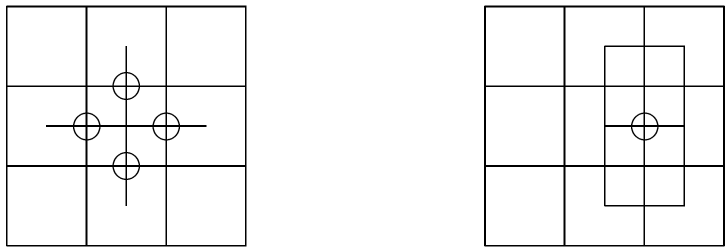

No-Flux Boundary Conditions

Instead of:

$$\begin{bmatrix} b & -b & & \\ -b & 1+b+c & -c & \\ & \ddots & \ddots & \ddots \\ & & & \end{bmatrix} \begin{bmatrix} u_1 \\ u_2 \\ \vdots \\ \\ \end{bmatrix}$$

Take:

$$\begin{matrix} -a \end{matrix} \begin{bmatrix} 1+a+b & -b & & \\ -b & 1+b+c & -c & \\ & \ddots & \ddots & \ddots \\ & & & \end{bmatrix} \begin{matrix} u_0 \\ \begin{bmatrix} u_1 \\ u_2 \\ \vdots \\ \\ \end{bmatrix} \end{matrix}$$

or with $u_0 = u_1$:

$$\begin{bmatrix} 1+b & -b & & \\ -b & 1+b+c & -c & \\ & \ddots & \ddots & \ddots \\ & & & \end{bmatrix} \begin{bmatrix} u_1 \\ u_2 \\ \vdots \\ \\ \end{bmatrix}$$

so PDE discretized *at the boundary.*

Otherwise, break in structure at boundary is dissipative and can create errors.

Semi-discrete Formulation

- Discrete diffusion operator:

$$h^{-2}G(\bar{U}_\sigma)\bar{U}$$

$\bar{U}_\sigma$ from $\bar{U}$ with $g = 1$ to time $\frac{1}{2}\sigma^2$, $\sigma \geq 0$.

- Initial value problem:

$$\begin{cases} \bar{U}' &= h^{-2}G(\bar{U}_\sigma)\bar{U} \\ \bar{U}(0) &= \bar{U}_0 \end{cases}$$

- Provided g regularized to be $\mathcal{C}^1$ [Weickert, 1998]:
  - Semi-discrete problem is well-posed!
  - Average grey level invariance:

$$\text{ave}\{\bar{U}(t)\} = \text{ave}\{\bar{U}(0)\}.$$

  - Extremem principle:

$$\min\{\bar{U}(0)\} \leq \bar{U}(t) \leq \max\{\bar{U}(t)\}$$

  - Smoothing Lyapunov Functionals:

ℓ_p norms, even moments, entropy.

  - Convergence to constant steady state:

$$\text{ave}\{\bar{U}(0)\}.$$

- Forthcoming work for g unbounded.

Fully Discrete Formulation

- Iterations: With $\mu = \tau/h^2$,

$$\text{Explicit:} \quad \bar{U}^{n+1} = [I + \mu G(\bar{U}^n_\sigma)]\bar{U}^n$$

$$\text{Semi-implicit:} \quad [I - \mu G(\bar{U}^n_\sigma)]\bar{U}^{n+1} = \bar{U}^n$$

- To satisfy extremum principle:
  - For Perona-Malik:
    - ▷ $g \leq 1$.
    - ▷ Explicit with $\mu \leq \frac{1}{2}$.
  - For g unbounded:
    - ▷ Use $g(\max\{\varepsilon, s\})$ or $g(\sqrt{\varepsilon^2 + s^2})$.
    - ▷ Explicit with $\mu \leq \frac{1}{2}\varepsilon^p$ too restrictive.
    - ▷ Semi-implicit with any $\mu > 0$.
- For semi-implicit scheme:
  - Use Jacobi preconditioned conjugate gradient.
    - ▷ Only a few iterations.
    - ▷ Very little extra computational expense.
  - Better than incomplete Cholesky, etc.
  - Actually need $\tilde{D} \approx D$ of $\left[I - \mu G(\bar{U}^n_\sigma)\right]$:

$$\tilde{D}_{i,j} = 1 + \frac{\mu}{2}\left(g_{i+\frac{1}{2},j+\frac{1}{2}} + g_{i-\frac{1}{2},j-\frac{1}{2}} + g_{i-\frac{1}{2},j+\frac{1}{2}} + g_{i+\frac{1}{2},j-\frac{1}{2}}\right)$$

Computational Results

1D results for Perona-Malik filters:

- Not all edges sharpened.
- First one best!
- λ small enough not to lose small slope edges.
- Larger λ sharpens steeper slopes.
- Staircasing for slopes larger than λ.
- Greater staircasing with smaller time steps.
- Course of image evolution:
  - Weaker edges sharpened earlier than stronger ones.
  - Sharpened edge disintegrates and blurs in relation to stronger neighbor.
  - Finally converges to constant steady state.
  - EXCEPT for finite precision fixed points.
- At $t_{\max}$ everything fairly stable.
- Only one accurate edge pair in each.
- Spatial regularization:
  - Rounds and reduces staircase steps.
  - Sufficient amount prevents staircasing.
  - Flattens small slope regions.
  - Retards edge sharpening.

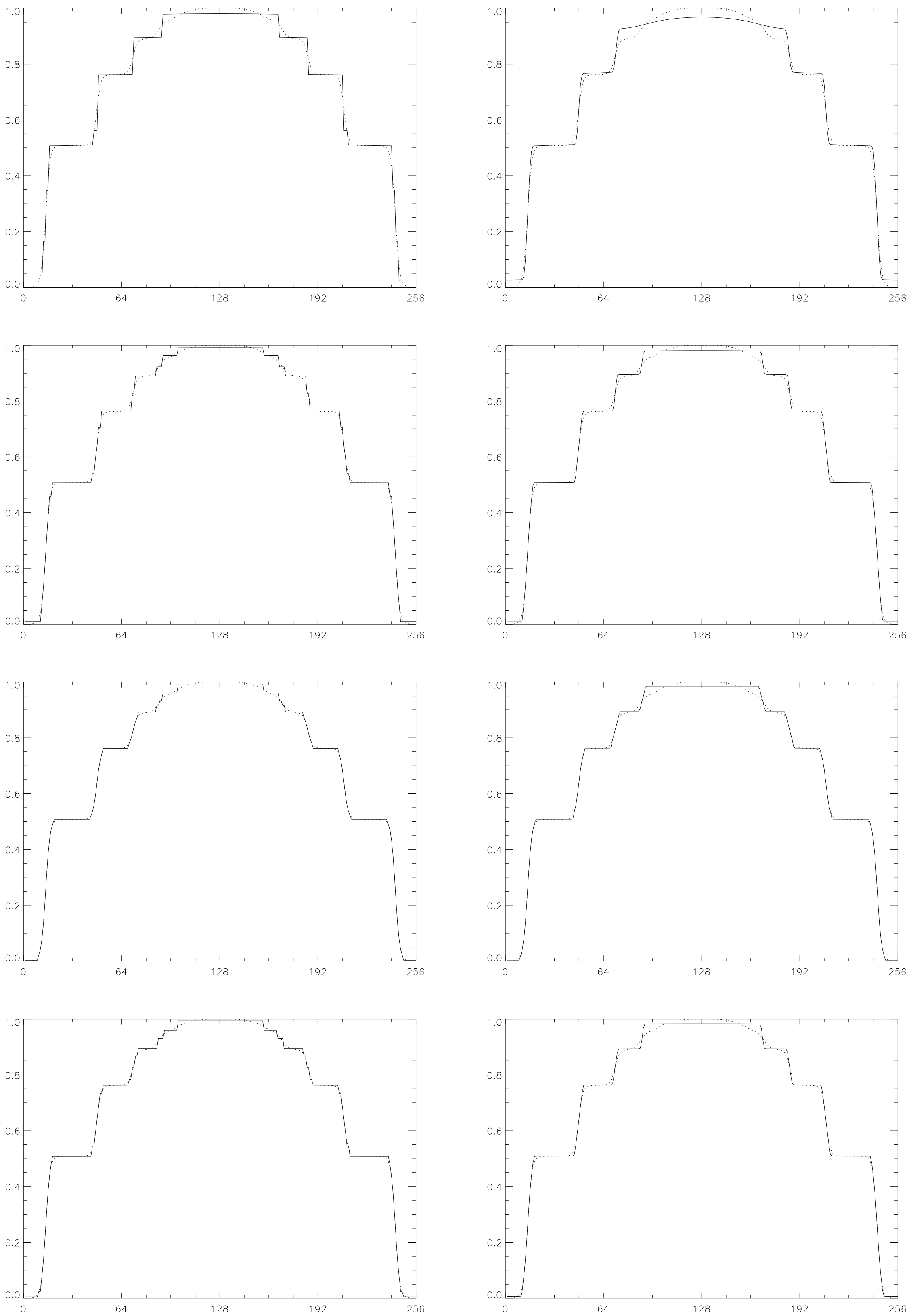

LEFT COLUMN: PM1, GR, PM2, and W.
RIGHT COLUMN: With spatial regularization.

1D results for BFB and GBFB filters:

- All edges sharpened well.
- BFB captures all inflection points correctly.
- GBFB misses only innermost pair by one cell.
- Course of evolution: very rapid and simultaneous sharpening.
- $\kappa = \lambda$ for GBFB.
- Larger κ gives:
  - slower sharpening,
  - progressively less accurate edges, and
  - eventually more staircasing.
- Greater staircasing with very small time steps.
- $t_{\max}$ same as for PM filters.
- More CG iterations reduce steps.
- Larger time steps and enough CG iterations sharpens any edge.
- Spatial regularization:
  - Same trends as with PM, but
  - One-step regularization only mildly rounds edges here for BFB.

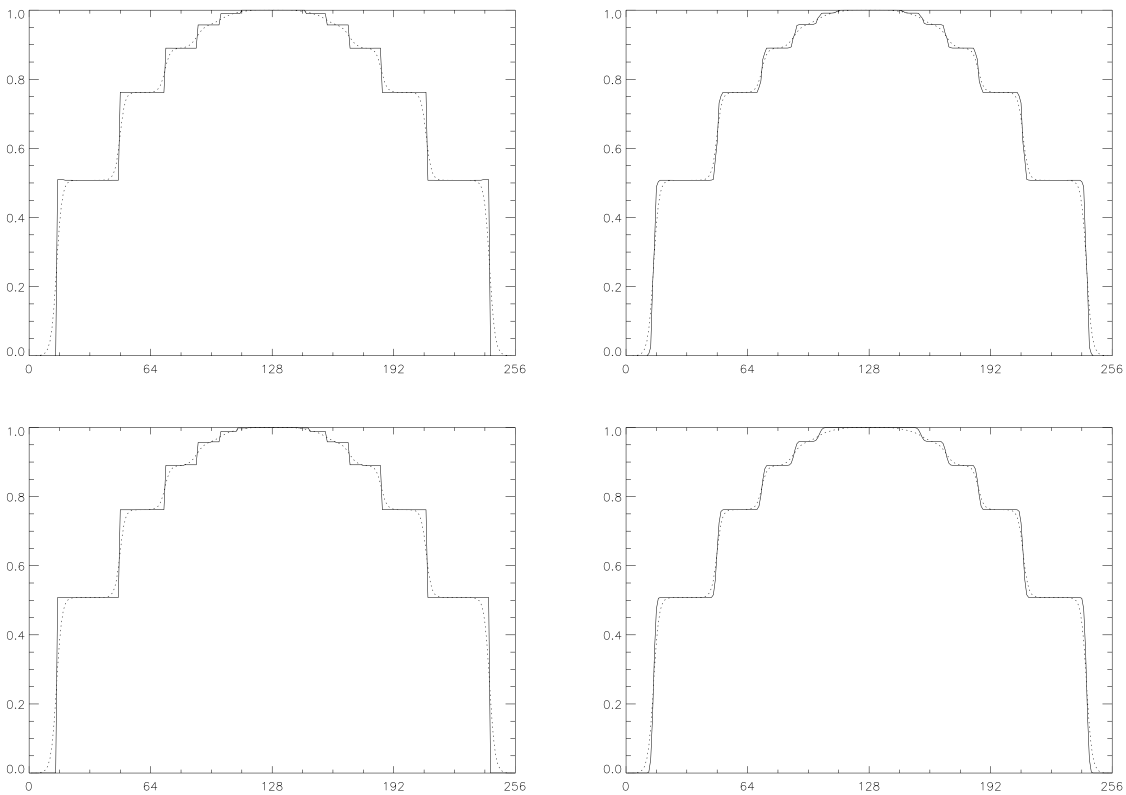

LEFT COLUMN: BFB and GBFB.
RIGHT COLUMN: With spatial regularization.

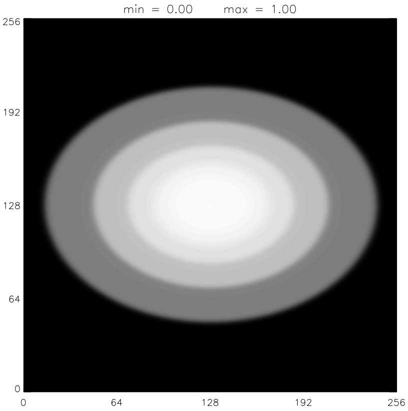

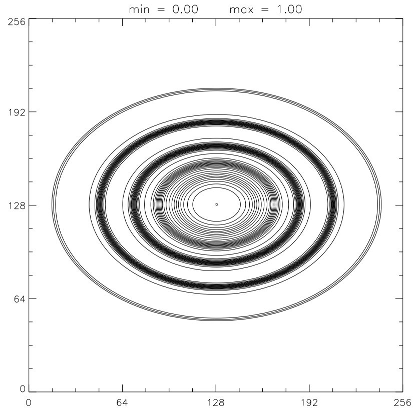

LEFT: region-filled contour of u_0.

RIGHT: lined contour plot of u_0 with levels $\{(i/i_{\max})^{1/4}\}$.

2D results for Perona-Malik filters:

- Not all edges sharpened.
- First one best!
- λ same as 1D not to lose small slope edges.
- Larger λ sharpens steeper slopes.
- Staircasing in spurious plateaus.
- Greater staircasing with smaller time steps.
- Course of image evolution: same as 1D but faster, tangential smoothing accelerates.
- At $t_{\max}$ slices look like 1D.
- Spatial regularization:
  - Sufficient amount prevents staircasing.
  - Flattens small slope regions.
  - Retards edge sharpening.
  - Rounds level curves.

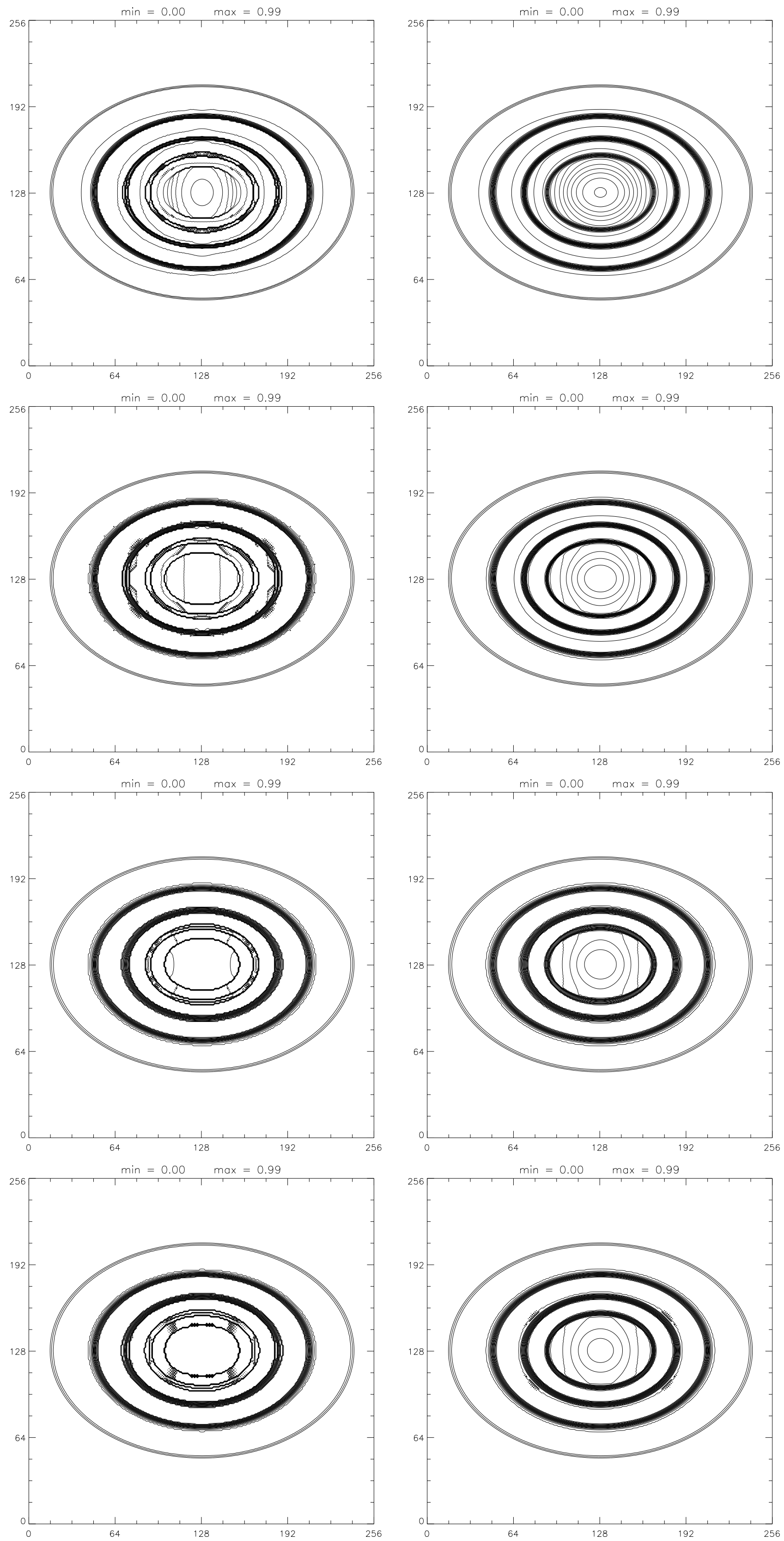

LEFT COLUMN: PM1, GR, PM2, and W.
RIGHT COLUMN: With spatial regularization.

2D results for BFB and GBFB filters:

- Aside from negligible contour variations, all edges sharpened well.
- BFB captures all inflection points:
  - correctly along diagonal lines,
  - within half a cell along horizontal and vertical lines.
- GBFB captures all inflection points within one cell along diagonal, horizontal, and vertical lines.
- Course of evolution: very rapid and simultaneous sharpening.
- $\kappa = \lambda$ for GBFB. Same κ trends.
- Greater staircasing with very small time steps.
- t_{max} same as for PM filters.
- Spatial regularization: same trends as earlier.

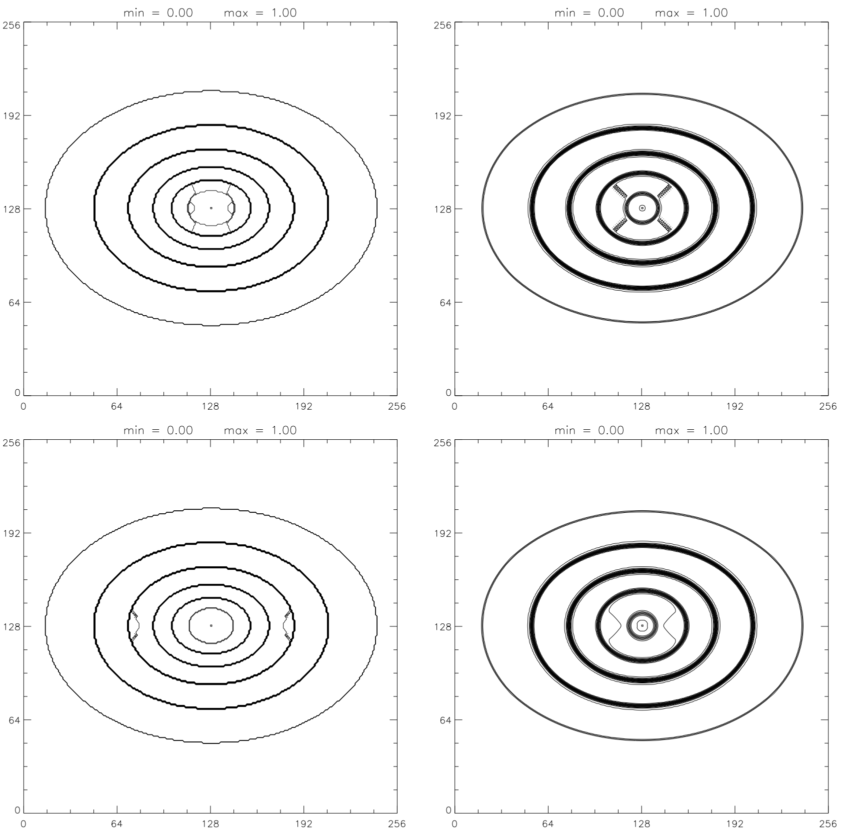

LEFT COLUMN: BFB and GBFB.
RIGHT COLUMN: With spatial regularization.

Comparison of PM2 and GBFB on MR image.

- Parameters just large enough to remove background noise.
- Staircasing in PM from normal smoothing.
- Decreasing λ enhances noise.
- GBFB reduces noise and preserves edges.
- Pure tangential smoothing very effective.
- As κ decreases:
  - Both tangential smoothing and normal sharpening increase.
  - Leads to segmentation-like results.
  - Eventually rounds level curves and enhances noise.
- Spatial regularization can treat noise enhancement but at aforementioned costs.

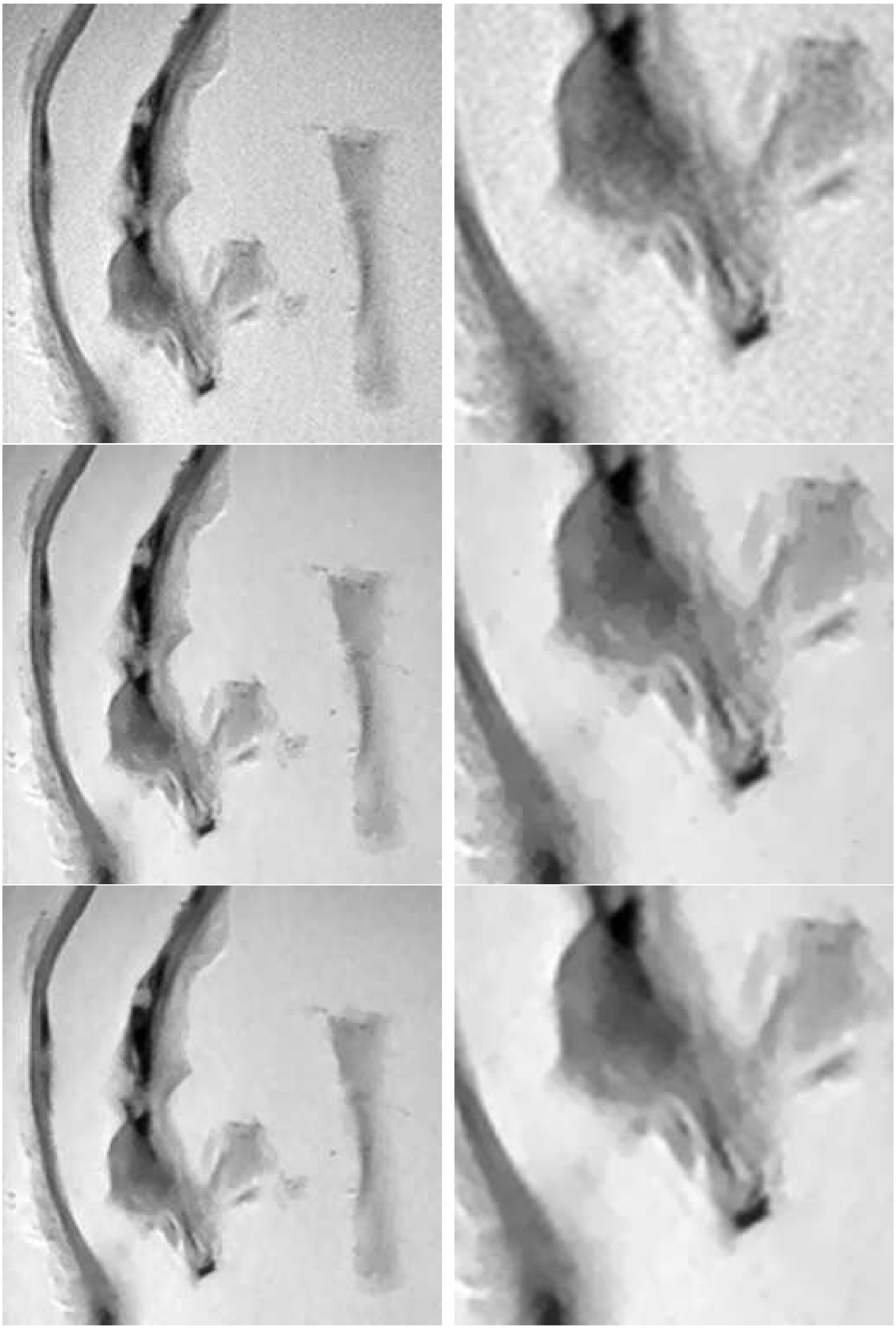

LEFT COLUMN: AS vessel MRI, PM2, and GBFB.
RIGHT COLUMN: Magnifications.